



## Article

# Natural Flavonoid Derivatives Have Pan-Coronavirus Antiviral Activity

Mattia Mori <sup>1,†</sup>, Deborah Quaglio <sup>2,†</sup>, Andrea Calcaterra <sup>2</sup>, Francesca Ghirga <sup>2</sup>, Leonardo Sorrentino <sup>3</sup>, Silvia Cammarone <sup>2</sup>, Matteo Fracella <sup>3</sup>, Alessandra D'Auria <sup>3</sup>, Federica Frasca <sup>3</sup>, Elena Criscuolo <sup>4</sup>, Nicola Clementi <sup>4,5</sup>, Nicasio Mancini <sup>4,5</sup>, Bruno Botta <sup>2</sup>, Guido Antonelli <sup>3</sup>, Alessandra Pierangeli <sup>3,‡</sup> and Carolina Scagnolari <sup>3,\*</sup>

<sup>1</sup> Department of Biotechnology, Chemistry and Pharmacy, University of Siena, 53100 Siena, Italy

<sup>2</sup> Department of Chemistry and Technologies of Drugs, Sapienza University of Rome, 00185 Rome, Italy

<sup>3</sup> Laboratory of Virology, Department of Molecular Medicine, Sapienza University of Rome, 00185 Rome, Italy

<sup>4</sup> Laboratory of Medical Microbiology and Virology, Vita-Salute San Raffaele University, 20132 Milan, Italy

<sup>5</sup> Laboratory of Medical Microbiology and Virology, IRCCS San Raffaele Hospital, 20132 Milan, Italy

\* Correspondence: carolina.scagnolari@uniroma1.it

† These authors contributed equally to this work.

‡ These authors contributed equally to this work.

**Abstract:** The SARS-CoV-2 protease (3CLpro) is one of the key targets for the development of efficacious drugs for COVID-19 treatment due to its essential role in the life cycle of the virus and exhibits high conservation among coronaviruses. Recent studies have shown that flavonoids, which are small natural molecules, have antiviral activity against coronaviruses (CoVs), including SARS-CoV-2. In this study, we identified the docking sites and binding affinity of several natural compounds, similar to flavonoids, and investigated their inhibitory activity towards 3CLpro enzymatic activity. The selected compounds were then tested *in vitro* for their cytotoxicity, for antiviral activity against SARS-CoV-2, and the replication of other coronaviruses in different cell lines. Our results showed that Baicalein (100 µg/mL) exerted strong 3CLpro activity inhibition (>90%), whereas Hispidulin and Morin displayed partial inhibition. Moreover, Baicalein, up to 25 µg/mL, hindered >50% of SARS-CoV-2 replication in Vero E6 cultures. Lastly, Baicalein displayed antiviral activity against alphacoronavirus (Feline-CoV) and betacoronavirus (Bovine-CoV and HCoV-OC43) in the cell lines. Our study confirmed the antiviral activity of Baicalein against SARS-CoV-2 and demonstrated clear evidence of its pan-coronaviral activity.

**Keywords:** baicalein; COVID-19; coronavirus



**Citation:** Mori, M.; Quaglio, D.; Calcaterra, A.; Ghirga, F.; Sorrentino, L.; Cammarone, S.; Fracella, M.; D'Auria, A.; Frasca, F.; Criscuolo, E.; et al. Natural Flavonoid Derivatives Have Pan-Coronavirus Antiviral Activity. *Microorganisms* **2023**, *11*, 314. <https://doi.org/10.3390/microorganisms11020314>

Academic Editor: Stefano Aquaro

Received: 27 December 2022

Revised: 17 January 2023

Accepted: 18 January 2023

Published: 25 January 2023



**Copyright:** © 2023 by the authors. Licensee MDPI, Basel, Switzerland. This article is an open access article distributed under the terms and conditions of the Creative Commons Attribution (CC BY) license (<https://creativecommons.org/licenses/by/4.0/>).

## 1. Introduction

The pandemic threat, caused by the severe acute respiratory syndrome coronavirus 2 (SARS-CoV-2), is still affecting people worldwide and viral variants contribute to the periodic rise in COVID-19 cases. Despite the development of multiple SARS-CoV-2 vaccines and the good degree of immunological protection achieved through vaccination, the mutation of newer variants and the uncertainty about how these detected mutations affect the efficacy of existing anti-spike vaccines have focused research on the development of efficacious drugs for COVID-19 therapeutic intervention.

COVID-19 emerged in late December 2019 [1,2] and subsequently SARS-CoV-2, a positive-strand RNA of the *Coronaviridae* family, was shown to be the cause. Based on numerous studies of the pathogenesis and virulence of coronavirus, distinct viral enzymes, namely 3-chymotrypsin-like cysteine protease (3CLpro), papain-like protease (PLpro), and RNA-dependent RNA polymerase (RDRP), were designated for exploring the potential of anti-SARS-CoV-2 drugs [3–5]. In particular, 3CLpro (also known as Mpro) plays a crucial role in viral protein maturation and antagonizes innate immunity [6]. Upon entry

into and the uncoating of the SARS-CoV-2 virions, the genomic RNA is translated into two polyproteins, PP1a and PP1ab, which are then cleaved into nonstructural proteins by PL2pro and 3CLpro viral proteases [6]. 3CLpro is responsible for cleaving at eleven sites on the polyproteins processing individual proteins, including the polymerase subunits [6]. Coronavirus 3CLpro remains one of the primary targets for SARS-CoV-2 therapeutics for the following reasons: (i) it has an indispensable role in the proteolytic processing of the viral RNA-polymerase complex, (ii) it is a highly conserved target protein, and (iii) it shares no structural similarity to human proteases [7].

Despite the intense efforts to develop SARS-CoV-2 specific inhibitors [8], only two antiviral agents, authorized by FDA in December 2021, have demonstrated activity in treating mild-to-moderate COVID-19 in patients who are at high risk of severe disease, including molnupiravir, an orally available base analogue that can be incorporated into RNA instead of cytidine triphosphate or uridine triphosphate, leading to mutated RNA products [9] and Paxlovid, a co-packaged combination of nirmatrelvir and ritonavir that acts as a peptidomimetic, covalent, and reversible inhibitor of 3CLpro [10]. The antiviral activity of nirmatrelvir has been reported to not be reduced when treating the SARS-CoV-2 variants Alpha (B.1.1.7), Beta (B.1.351), Gamma (P.1), Delta (B.1.617.2), and Omicron (B.1.1.529) [11], confirming the conservation of the sequence of this enzyme among coronaviruses. Regrettably, cases of patients experiencing a rebound in SARS-CoV-2 viral load and symptoms after completing Paxlovid treatment have been documented [12]. Thus, the development of antiviral therapies directed against viral targets with minimal side effects remains highly urgent.

In the search for additional therapeutic options, several studies conducted *in silico*, *in vitro*, and *in vivo* showed that small natural molecules belonging to polyphenol family [13,14] have the potential to hinder various steps of coronavirus replication. Furthermore, growing understanding of the possible antiviral mechanisms of flavonoids based on previous studies with other coronaviruses, including SARS-CoV-2 [15], and the potential activity of flavonoids to ameliorate post-COVID-19 syndrome through their anti-inflammatory properties [16–18] underline the relevance of further exploring the anti-coronavirus activities of these compounds.

To that end, molecular docking was used to screen and determine the docking patterns and binding affinities of compounds with structural similarities to flavonoids, which are the major targets of SARS-CoV-2 3CLpro [19]. Then, an enzymatic assay was employed in order to examine the inhibitory effects of these compounds on 3CLpro. The activity of selected 3CLpro inhibitors in the life cycle of coronavirus was then assessed by evaluating their antiviral activity against SARS-CoV-2 and different alpha (Feline-CoV) and beta coronaviruses (Bovine-CoV and HumanCoV-OC43) *in vitro*.

## 2. Methods

### 2.1. Study Design

Two Flavonoids (Luteolin and 7,8-hydroxyflavone) have previously been found to be active against 3CLpro [20]. Other compounds with structural analogy were tested through *in silico* analyses for possible activity against 3CLpro. The compounds that were found to be active *in silico* were tested through enzymatic assays. Then, the compounds that were found to be active were tested through an *in vitro* assay for anti-SARS-CoV-2 activity. Lastly, in order to investigate possible anti-pan-coronaviral activity, we evaluated these compounds against Feline (F)-CoV, Bovine (B)-CoV, and Human (H)CoV-OC43.

### 2.2. Chemistry

All the tested compounds (1–12) (Table 1) are known structures belonging to the in-house library of natural products available from the Organic Chemistry Laboratory of the Department of Chemistry and Technology of Drugs of Sapienza University of Rome, Italy [21]. The chemical identity of the compounds was assessed by re-running NMR experiments and proved to be in agreement with the literature data reported below for each

compound. The purity of all the compounds, checked by reversed-phase High-Performance Liquid Chromatography (HPLC), was always higher than 95%.

**Table 1.** Flavonoid family compounds.

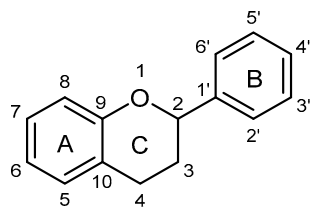
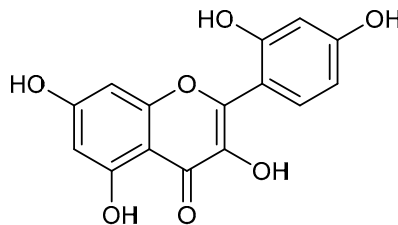
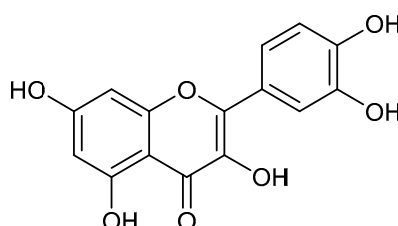
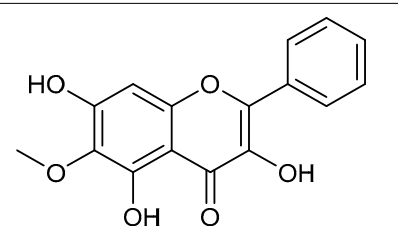
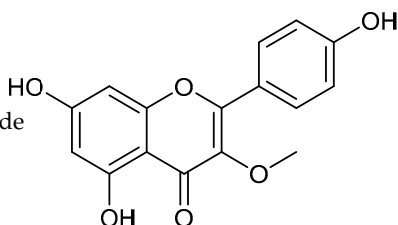
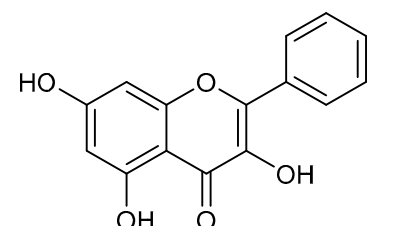
Mol.	Common Name	Chemical Structure	M.W.	Molecular Formula	Source	Reference
 <p>Basic Flavonoid Skeleton</p>						
Flavanones						
1	Morin		302.24	C <sub>15</sub> H <sub>10</sub> O <sub>7</sub>	Moriaceae family	[22]
2	Quercetin		302.24	C <sub>15</sub> H <sub>10</sub> O <sub>7</sub>	<i>Ginkgo biloba</i> (Ginkgoaceae family) <i>Hypericum perforatum</i> (Hypericaceae family) <i>Sambucus canadensis</i> (Adoxaceae family)	[23,24]
3	Alnusin		300.27	C <sub>16</sub> H <sub>12</sub> O <sub>6</sub>	<i>Xerochrysum viscosum</i> (Asteraceae family) <i>Alnus sieboldiana</i> (Betulaceae family)	[25]
4	Isokaempferide		300.27	C <sub>16</sub> H <sub>12</sub> O <sub>6</sub>	<i>Amburana cearensis</i> (Fabaceae family)	[26]
5	Galangin		270.24	C <sub>15</sub> H <sub>10</sub> O <sub>5</sub>	<i>Alpinia officinarum</i> (Zingiberaceae family) <i>Helichrysum aureonitens</i> (Asteraceae family) <i>Alpinia galanga</i> (Zingiberaceae family)	[27–29]

Table 1. Cont.

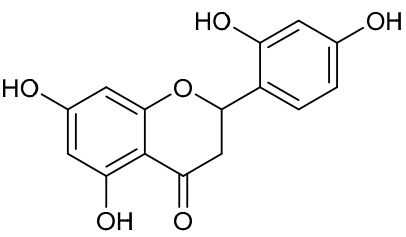
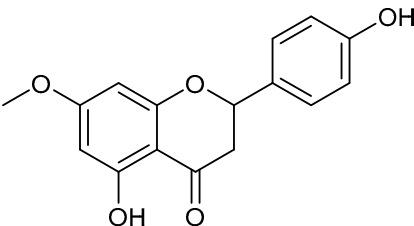
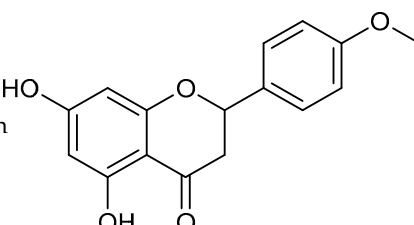
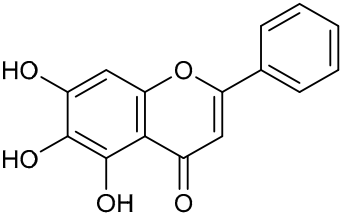
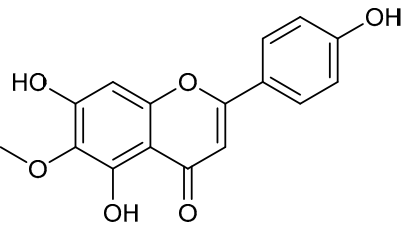
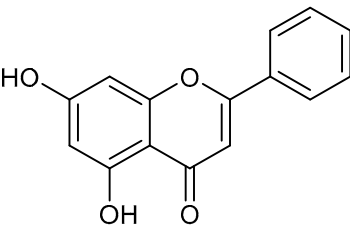
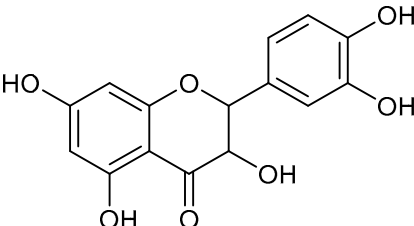
Flavanones						
6	Steppogenin		288.26	C <sub>15</sub> H <sub>12</sub> O <sub>6</sub>	<i>Euphorbia nicaeensis</i> (Euforbiaceae family) <i>Maclura tricuspidata</i> (Moraceae family)	[30]
7	Sakuranetin		286.28	C <sub>16</sub> H <sub>14</sub> O <sub>5</sub>	<i>Polymnia fruticosa</i> (Araliaceae family)	[31]
8	Isosakuranetin		286.28	C <sub>16</sub> H <sub>14</sub> O <sub>5</sub>	<i>Monarda didyma</i> (Lamiaceae family)	[32]
Flavones						
9	Baicalein		270.24	C <sub>15</sub> H <sub>10</sub> O <sub>5</sub>	<i>Scutellaria baicalensis</i> (Lamiaceae family)	[33]
10	Hispidulin		300.27	C <sub>16</sub> H <sub>12</sub> O <sub>6</sub>	<i>Crossostephium chinense</i> , <i>Grindelia argentina</i> and <i>Saussurea involucrate</i> (Asteraceae family) <i>Arrabidaea chica</i> (Bignoniaceae Family)	[34,35]
11	Chrysin		254.24	C <sub>15</sub> H <sub>10</sub> O <sub>4</sub>	<i>Passiflora caerulea</i> and <i>Passiflora incarnata</i> (Passifloraceae family) <i>Oroxylum indicum</i> (Bignoniaceae family)	[36]

Table 1. Cont.

		Flavanonol			
12	Taxifolin		304.25	C <sub>15</sub> H <sub>12</sub> O <sub>7</sub>	<i>Pinus roxburghii</i> , <i>Cedrus deodara</i> (Pinaceae family) [37]

Compound 1 (Morin or 2-(2,4-dihydroxyphenyl)-3,5,7-trihydroxy-4H-chromen-4-one) showed NMR spectra identical to those reported in the literature [38]. Compound 2 (Quercetin or 2-(3,4-dihydroxyphenyl)-3,5,7-trihydroxy-4H-chromen-4-one) showed NMR spectra identical to those reported in the literature [39]. Compound 3 (Alnusin or 3,5,7-trihydroxy-6-methoxy-2-phenyl-4H-chromen-4-one) showed NMR spectra identical to those reported in the literature [40]. Compound 4 (Isokaempferide or 5,7-dihydroxy-2-(4-hydroxyphenyl)-3-methoxy-4H-chromen-4-one) showed NMR spectra identical to those reported in the literature [41]. Compound 5 (Galingin or 3,5,7-trihydroxy-2-phenyl-4H-chromen-4-one) showed NMR spectra identical to those reported in the literature [42]. Compound 6 (Steppogenin or 2-(2,4-dihydroxyphenyl)-5,7-dihydroxychroman-4-one) showed NMR spectra identical to those reported in the literature [43]. Compound 7 (Sakuranetin or 5-hydroxy-2-(4-hydroxyphenyl)-7-methoxychroman-4-one) showed NMR spectra identical to those reported in the literature [44]. Compound 8 (Isosakuranetin or 5,7-dihydroxy-2-(4-methoxyphenyl)chroman-4-one) showed NMR spectra identical to those reported in the literature [45]. Compound 9 (Baicalein or 5,6,7-trihydroxy-2-phenyl-4H-chromen-4-one) showed NMR spectra identical to those reported in the literature [46]. Compound 10 (Hispidulin or 5,7-dihydroxy-2-(4-hydroxyphenyl)-6-methoxy-4H-chromen-4-one) showed NMR spectra identical to those reported in the literature [47]. Compound 11 (Chrysin or 5,7-dihydroxy-2-phenyl-4H-chromen-4-one) showed NMR spectra identical to those reported in the literature [48]. Compound 12 (Taxifolin or 2-(3,4-dihydroxyphenyl)-3,5,7-trihydroxychroman-4-one) showed NMR spectra identical to those reported in the literature [49].

### 2.3. In Silico Screening of Natural Compounds

The crystallographic structure of SARS-CoV-2 3CLpro in complex with a small molecular fragment at 1.95 Å resolution and coded by PDB-ID: 5R81 was selected [50]. In order to relax possible structural constraints, 500 ns of MD simulations were run with AMBER18 using the ff14SB force field for the protein and GAFF for the small molecule. An already validated protocol for classical MD simulations was used [51–53]. A representative structure was extracted from the MD trajectory using a cluster analysis, and it was used as a rigid receptor in the subsequent structure-based virtual screening of a proprietary library of natural products [21]. Virtual screening was carried out with the FRED docking program, version 3.3.0.3 (OpenEye Scientific Software) [54,55], in a binding site of 390 Å<sup>3</sup> that was centered on the binding pose of the crystallographic ligand. For virtual screening purposes, 3D conformers of natural products included in the proprietary library were generated from SMILES using the OMEGA software version 3.1.0.3 (OpenEye Scientific Software) [56], whereas the protonation state at a pH of 7.4 was assigned using QUACPAC version 2.0.0.3 (OpenEye Scientific Software) [57]. Ligand energy minimization was carried out using SZYBKI, version 1.10.0.3 (OpenEye Scientific Software) [58], using the MMFF94S force field.

### 2.4. SARS-CoV-2 3CLpro Assay

In order to examine the compounds with structural analogies to active flavonoids 7,8-Hydroxyflavone and Luteolin for their inhibitory activity against SARS-CoV-2, a preliminary screening using an enzymatic assay [3CLpro, Untagged SARS-CoV-2 Kit, AMSBio (Abingdon, UK) was performed. We tested the compounds at different concentrations and the control inhibitor compounds were incubated with 3CLpro for 30 min, following the manufacturer's instructions. Subsequently, the substrate of protease was added, and after 4 h of incubation, the fluorescence intensity following the cleavage of the enzyme substrate was measured at an excitation wavelength of 360 nm and an emission wavelength of 460 nm. The "blank" value (fluorescence intensity of the substrate in an assay buffer) was subtracted from each reading and the percentage of inhibition shown by each compound was calculated with respect to untreated 3CLpro activity (0%) and to the control inhibitor compound (100%). All the conditions were performed in triplicate.

### 2.5. Cell Viability Assay to Determine Compounds' Toxicity

Cell viability was assessed using the Cell Proliferation kit II (XTT) (Roche Diagnostics, Merck, Darmstadt, Germany) as previously described [59]. In this assay, the tetrazolium salt 2,3-bis-(2-methoxy-4-nitro-5-sulphophenyl)-2H-tetrazolium-5-carboxanilide (XTT) was cleaved by viable cells in order to form an orange formazan dye that is then quantified photometrically at 450 nm. Briefly, the cells ( $4 \times 10^5$  cells/mL) were cultured in 96-well plates for 24 h. The culture medium was then replaced by medium containing serial dilutions of the 3CLpro inhibitors, and the cells were incubated for 24, 48, 72, and 96 h. Then, XTT was added to each well and the plates were incubated for 2 h. Optical density was measured at 450 nm (reference wavelength—650 nm) using a Multiskan GO plate reader (Thermo Scientific Instruments, Waltham, MA, USA). For the quantifications, the background levels of media without cultured cells were subtracted.

### 2.6. SARS-CoV-2 In Vitro Assay

Vero E6 (Vero C1008, clone E6—CRL-1586; ATCC) cells were cultured in Dulbecco's Modified Eagle Medium (DMEM) supplemented with non-essential amino acids (NEAA), penicillin/streptomycin (P/S), Hepes buffer, and 10% (*v/v*) Fetal bovine serum (FBS). A clinical isolate of SARS-CoV-2 Omicron BA.5 (hCoV-19/Italy/LOM-UniSR38/2022, GISAID ID: EPI\_ISL\_15778241) was obtained and propagated in Vero E6 cells, and the viral titer was determined by the 50% tissue culture infective dose (TCID<sub>50</sub>) and plaque assay. All the infection experiments were performed in a biosafety level three (BSL-3) laboratory, as previously described [59].

### 2.7. SARS-CoV-2 Titration

Virus stocks were titrated using the Endpoint Dilutions Assay (EDA, TCID<sub>50</sub>/mL), as described [59]. Briefly, Vero E6 cells ( $4 \times 10^5$  cells/mL) were seeded into 96 wells plates and infected with base 10 dilutions of the virus stock. After 1 h of adsorption at 37 °C, the cell-free virus was removed, and complete medium was added to the cells after a PBS wash. After 72 h, the cells were observed to evaluate CPE. The Reed and Muench method was used to calculate the 50% endpoint using serial dilutions.

### 2.8. Feline-CoV, Bovine-CoV, and HCoV-OC43 In Vitro Assays and Titration

HRT-18 (CCL-244; ATCC) and CRFK (CCL-94; ATCC) cells were cultured in DMEM supplemented with NEAA, P/S, Hepes buffer, and 10% FBS. A clinical isolate of F-CoV (kind gift from Prof. Buonavoglia, University of Bari) was obtained and propagated in CRFK cells, whereas B-CoV (kind gift from Prof. Buonavoglia, University of Bari) was isolated and propagated in HRT-18 cells. HCoV-OC43 was a kind gift from Prof. Baldanti (S. Matteo Hospital, Pavia). A titer of each CoV was measured using RT/Real-Time PCR assays, as previously described [60]. Briefly, the following primers and probes were used [60]: F-CoV (Forward: 5'-GATTTGATTTGGCAATGCTAGATTT-3'; Reverse: 5'-AACAACTACTAGATCCAGACGTTAGCT-3'; Probe: 5'-6FAM/TCCATTGTTG GCTCGTCATAGCGGA/TAM-3'), B-CoV (Forward: 5'-CTGGAAGTTGGTGGAGTT-3'; Reverse: 5'-ATTATCGGCCTAACATACATC-3'; Probe: 5'-6FAM/CCTTCATATCTATACA CATCAAGTTGTT/TAM-3'), and HCoV-OC43 (Forward: 5'-AGCAGACCTTCCTGAGCC TTCAAT-3'; Reverse: 5'-AGCAACCAGGCTGATGTCAATACC-3'; Probe: 5'-/6FAM/TGA CATTGTTCGATCGGGACCCAAGTA/36-TAMSp/-3').

### 2.9. Coronaviruses In Vitro Assays

The cells ( $4 \times 10^5$  cells/mL) were seeded into 96-well plates 24 h prior to the experiment. The cells were pretreated with different concentrations of selected 3CLpro inhibitors (1:2 serial dilutions) for 1 h at 37 °C, and were then infected for 1 h with each CoV (0.1 multiplicity of infection, MOI) in the presence of each compound. After a PBS wash to remove cell-free virus particles, 3CLpro-inhibitor-containing medium with 2% FBS was added to the cells and was maintained until the end of the experiment [48 h post-infection (hpi)]

for F-CoV (CRFK), 72 hpi for SARS-CoV-2 (Vero E6), and 96 hpi for B-CoV (HRT-18) and HCoV-OC43 (HRT-18)]. Then, the SARS-CoV-2 cytopathic effect (CPE) was assessed using a scoring system (0 = uninfected; 0.5 to 2.5 = increasing number/area of plaques; 3 = all the cells are infected), as described [59]. The infection control (score 3) was set as 100% infection and the uninfected cells (score 0) were set as 0% infection. The whole surface of the wells was considered for the analysis (5× magnification). F-CoV, B-CoV, and HCoV-OC43 titers were evaluated through RT/Real-Time PCR and absolute quantifications were calculated using a standard curve [60]. All the conditions were tested in triplicate.

### 2.10. Statistical Analysis

A two-way ANOVA and Dunnett's multiple comparisons test were performed for cell viability assessment. The CPE observed was normalized to corresponding SARS-CoV-2 infection control. Then, a two-way ANOVA and Tukey's multiple comparisons test was performed for the evaluation of CPE scoring results (GraphPad Prism 8). The antiviral activity of the compounds tested against F-CoV, B-CoV, and HCoV-OC43 were calculated as the percentage of the reduction of viral RNA copies between untreated infected cells and treated infected cells. A *p*-value below 0.05 was considered significant.

## 3. Results

### 3.1. Virtual Screening of the in-House Natural Products Library

The natural products included in the in-house library (available at Sapienza University of Rome in the research group of Prof. Bruno Botta [21]) were prepared for virtual screening through (i) the generation of 3D conformers, (ii) ionization at a pH of 7.4, and (iii) energy minimization in water solvent with the MMFF94S force field. The crystallographic structure of SARS-CoV-2 3CLpro in complex with the non-covalent inhibitor Z1367324110 (PDB ID: 5R81) was selected as a receptor in structure-based virtual screening [49]. To remove any possible structural bias from protein crystallization, molecular dynamics (MD) simulations were carried out on the 3CL/Z1367324110 crystallographic complex using a previously validated protocol. After 500 ns of unrestrained production of the MD trajectories, the MD frames were clustered using a hierarchical agglomerative algorithm, and the centroid frame of the most populated cluster was selected as representative structure for subsequent structure-based virtual screening.

Virtual screening was performed by molecular docking simulations with a FRED docking program [50–52]. Coupling visual inspection of the binding modes with analysis of the Chemgauss4 score led to the selection of 12 small molecules as candidate inhibitors of SARS-CoV-2 3CLpro. All the identified compounds are plant polyphenolic secondary metabolites belonging to the flavonoid family (Table 1). The basic flavonoid structure exists in a diphenylpropane skeleton (C6–C3–C6), namely the flavan nucleus, where two benzene rings (ring A and B) are linked by a three-carbon chain forming a pyran ring C (Table 1). Based on the degree of unsaturation and the oxidation level of ring C, they can be divided in different subclasses: Morin (1), Quercetin (2), Alnusin (3), Isokaempferide (4), and Galangin (5) are flavonols featuring a 3-hydroxyflavone backbone structure; Steppogenin (6), Sakuranetin (7), and Isosakuranetin (8) are flavanones featuring a flavan backbone; Baicalein (9), Hispidulin (10), and Chrysin (11) are flavones; and Taxifolin (12), which features a 3-hydroxyflavanone backbone, is a flavanonol.

### 3.2. SARS-CoV-2 3CLpro Assay

We evaluated the inhibitory activity of compounds 1–12 against the 3CLpro of SARS-CoV-2 in on-plate enzymatic assays at the following concentrations: 100 µg/mL and serial 1:2 dilutions reaching a final concentration of 0.78 µg/mL. We observed substantial inhibitory activity of Baicalein (94.72%) at the concentration of 100 µg/mL (Table 2), whereas for Hispidulin and Morin, partial inhibition of the protease activity was observed at 100 µg/mL (55.62% and 53.64%, respectively) (Table 2). Isokaempferide exhibited a detectable effect on 3CLpro when used at concentrations ranging from 100 µg/mL to

25 µg/mL, leading to a percentage of reduction of its activity of 49.98%, 40.06%, and 19.69%, respectively. We also examined the inhibitor effects of Luteolin and 7,8-dihydroxyflavone, for which antiviral activity has been previously reported [20,61], finding low activity against 3CLpro at 100 µg/mL (38.12% and 39.80%, respectively), and undetectable activity at 25 µg/mL (Table 2). By contrast, no activity against 3CLpro was observed for Taxifolin, Steppogenin, Quercetin, Chrysin, Sakuranetin, Alnusin, Galangin, and Isosakuranetin when used at concentrations ranging from 100 µg/mL to 6.125 µg/mL (data not shown).

**Table 2.** Enzymatic anti-3CLpro activity of selected compounds.

Compound	Molecular Model	Concentrations Tested (µg/mL)	Percentage of Inhibition of 3CLpro
Morin	Docking	100.00	53.64 (33.85)
		50.00	18.64 (4.36)
		25.00	<10
		12.5	<10
Baicalein	Docking	100.00	94.72 (9.11)
		50.00	72.14 (7.75)
		25.00	25.57 (6.67)
		12.5	17.28 (1.11)
Hispidulin	Docking	100.00	55.62 (17.04)
		50.00	29.76 (12.56)
		25.00	<10
Luteolin	Docking	12.5	<10
		100.00	38.12 (2.32)
		50.00	30.88 (3.53)
		25.00	<10
7,8-Dihydroxy-flavone	Docking	12.5	<10
		100.00	39.8 (0.31)
		50.00	34.54 (0.13)
		25.00	<10
Isokaempferide	Cluster	12.5	<10
		50.00	49.98 (22.38)
		25.00	40.06 (27.12)
		12.5	19.69 (13.71)

Data of the inhibition percentage of 3CLpro activity are shown as a mean of the three experiments (standard deviations).

Given the Morin, Baicalein, Hispidulin, and Isokaempferide had detectable activity against SARS-CoV-2 3CLpro, we investigated the efficacy of these compounds in the impairment of SARS-CoV-2 replication on Vero E6 cells with an in vitro assay.

### 3.3. Effect of the 3CLpro Inhibitors on VERO E6 Viability

Vero E6 cells were tested with serial dilutions of Morin, Baicalein, Hispidulin, Isokaempferide, Luteolin, and 7,8-dihydroxyflavone in order to assess their cytotoxicity. The results showed no difference between the treated and untreated cells when Baicalein and Morin were used, even after testing higher concentrations for 72 h (Figure 1A,B). Instead, the other compounds induced some degree of cytotoxicity. In detail, Hispidulin (Figure 1C) was found to be toxic when used at 50 µg/mL after 24 and 48 h ( $p < 0.0001$  and  $p < 0.01$ , respectively) and at 25 µg/mL after 72 h of treatment ( $p < 0.01$ ). Luteolin (Figure 1D) impaired cell viability starting from 12.5 µg/mL at each considered time point ( $p < 0.001$  after 48 and 72 h,  $p < 0.01$  after 24 h), as well as Isokaempferide (Figure 1E) starting from 50 µg/mL ( $p < 0.001$  at all the time points), and 7,8-dihydroxy-flavone starting from 6.25 µg/mL ( $p < 0.0001$ ) at all the time points.

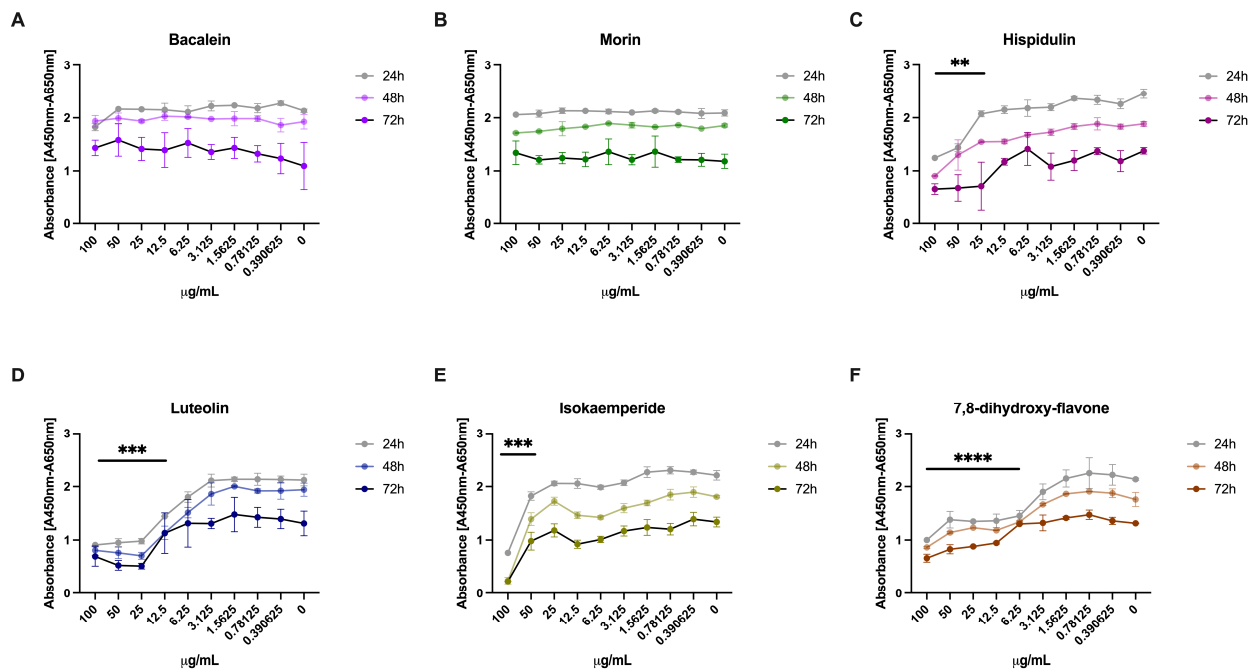


**Figure 1.** Cell viability analysis. Different concentrations (100–0.4 µg/mL) of the selected 3CLpro inhibitors (A–F) were tested in order to assess their toxicity on Vero E6. Absorbance was reported as mean values  $\pm$  SD, \*\*  $p < 0.01$ , \*\*\*  $p < 0.001$ , and \*\*\*\*  $p < 0.0001$ .

### 3.4. Antiviral Activity of 3CLpro Inhibitors against SARS-CoV-2

Vero E6 cells were treated with serial dilutions of the selected compounds, relying on cell viability data to determine the highest concentrations to test: 100 µg/mL for Baicalein and Morin (Figure 2A,B), 25 µg/mL for Hispidulin (Figure 2C), 10 µg/mL for Luteolin and 7,8-dihydroxy-flavone (Figure 2D,F), and 50 µg/mL for Isokaempferide (Figure 2E). The inhibitors were added one hour before inoculation with the SARS-CoV-2 Omicron BA.5 variant (0.1 Multiplicity of infection, MOI), and were monitored for cytopathic effects at 72 hpi. The results showed that no compound, at any concentration, could fully protect the cells from infection with the virus. Only the treatment with Baicalein hindered virus replication above 50%, starting from a concentration of 25 µg/mL.

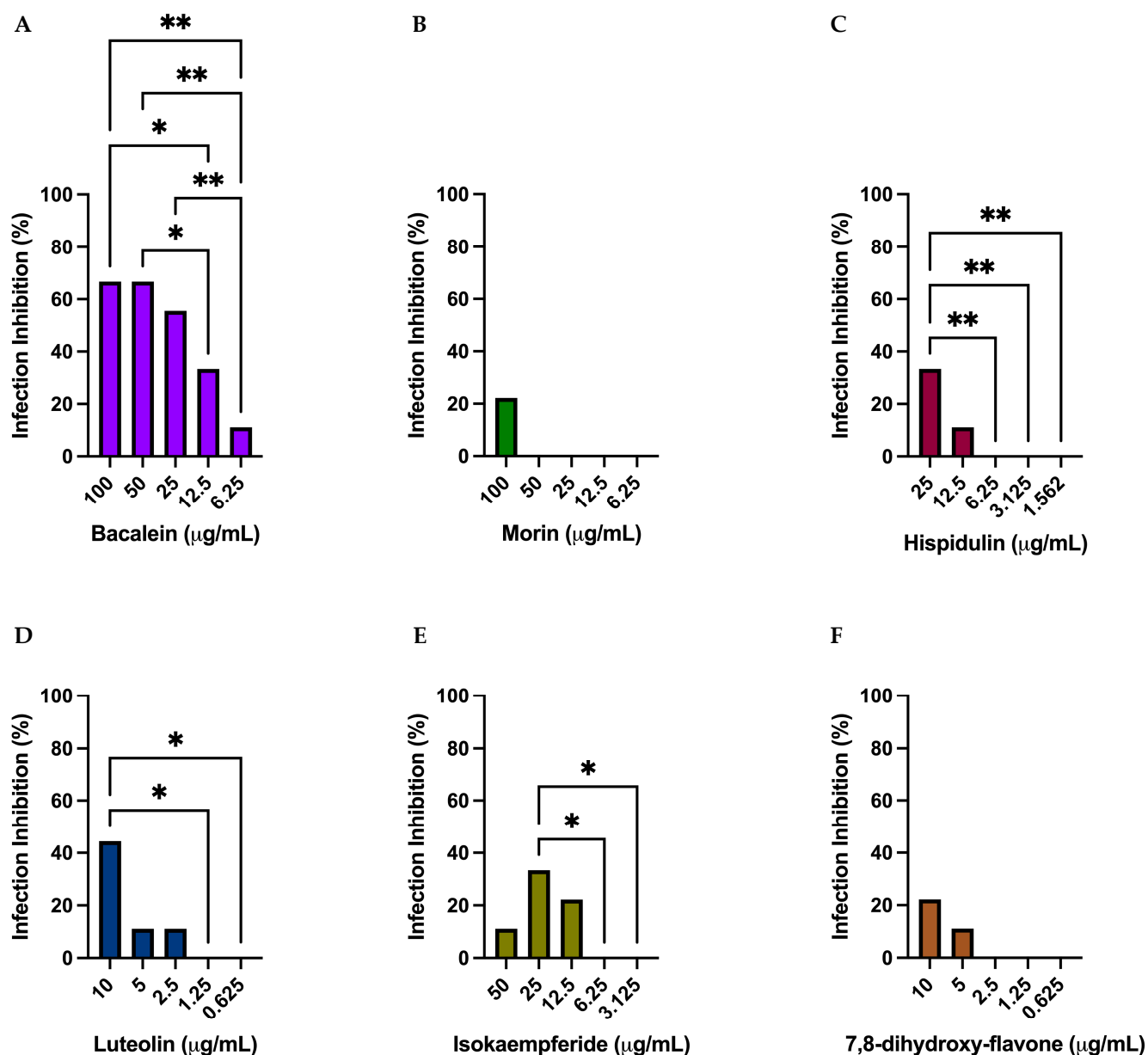


**Figure 2.** (A–F) Antiviral activity of selected 3CLpro inhibitors. The inhibition of Omicron BA.5 infection was tested using different concentrations of the selected compounds and was assessed at 72 hpi. Mean values are reported for all the experimental replicates. Standard deviations were less than 10% of the mean values. An ordinary one-way ANOVA with a Tukey’s multiple comparisons test, with a single pooled variance, was performed. \*  $p < 0.05$  and \*\*  $p < 0.01$ .

### 3.5. Effect of the 3CLpro Inhibitors on CRFK and HRT-18 Viability and Pan-Coronaviral Activity

In order to investigate possible anti-pan-coronaviral activity, we tested the efficacy of Baicalein and Luteolin against Feline-CoV (F-CoV), Bovine-CoV (B-CoV) and human-CoV (HCoV) OC43 replication.

CRFK and HRT-18 were tested with serial dilutions of Baicalein and Luteolin in order to assess their cytotoxicity. The highest concentrations with no toxic activity were 50 µg/mL for Baicalein and 3.125 µg/mL for Luteolin in both the cell lines. In order to test pan-coronavirus antiviral activity, Baicalein and Luteolin were added 1 h before inoculation with F-CoV on CRFK cells, B-CoV, and HCoV-OC43 on HRT-18 cells (0.1, Multiplicity of infection, MOI) and were monitored 48 hpi (F-CoV) and 96 hpi (B-CoV and HCoV-OC43). Only Baicalein showed antiviral activity (Table 3); it inhibited F-CoV and

B-CoV at 50 µg/mL and at lower concentrations (up to 12.5 µg/mL) inhibited HCoV-OC43 replication (Table 3).

**Table 3.** Pan-coronavirus antiviral activity of Baicalein.

Compound	Concentrations Tested (µg/mL)	Antiviral Activity against F-CoV	Antiviral Activity against B-CoV	Antiviral Activity against OC43
Baicalein	100	TX	TX	TX
	50	66.73	99.60	99.99
	25	<50	89.85	99.99
	12.5	<50	<50	99.98
	6.25	<50	<50	<50
	3.125	<50	<50	<50
	1.56	<50	<50	<50
	0.78	<50	<50	<50

Data are expressed as a percentage. Antiviral activity is expressed as  $1-(1/10LRV) * 100$ . All the experiments were performed in triplicate. Standard deviations were less than 10% of the mean values. TX: Toxic; LRV: Log Reduction Value.

### 3.6. Predicted Binding Mode of Most Effective SARS-CoV-2 3CLpro Inhibitors

The possible binding mode of the bioactive compounds discussed above within the catalytic site of SARS-CoV-2 3CLpro was investigated by molecular docking simulations. Since all the docked compounds are members of the flavone family, although they bear different substitution patterns, it is not surprising that they bind within the catalytic site of SARS-CoV-2 3CLpro in a highly consistent manner to each other, as well as to the docking-based binding mode of other flavonoids from the literature [62]. Specifically, Morin, Luteolin, and the 7,8-dihydroxyflavone bind with opposite orientations with respect to Baicalein, Hispidulin, and Isokaempferide. The latter of these have the polyhydroxylated ring A of the flavone scaffold projected to the inner core of 3CLpro that is in the proximity of Asn142 (Figure 3). Besides stacking to the side chain of His41, the natural compounds establish H-bond interactions with the backbone of Asn142 (Baicalein, Isokaempferide, and Morin), with the phenolic side chain of Try54 (Luteolin), with the backbone of Gln189 (Morin and Luteolin), with the backbone of Thr190 (Morin, Hispidulin, and Luteolin), and with the side chain of Cys44. Only 7,8-dihydroxyflavone establishes an H-bond interaction with the side chain of Glu166 (Figure 3). Notably, Baicalein and Hispidulin are able to H-bond a water molecule, which was identified by the MD simulations and is found in X-ray structures (Figure 3A,C).

The predicted binding mode supports the inhibition of SARS-CoV-2 3CLpro by these natural compounds, as was confirmed by the experimental studies.

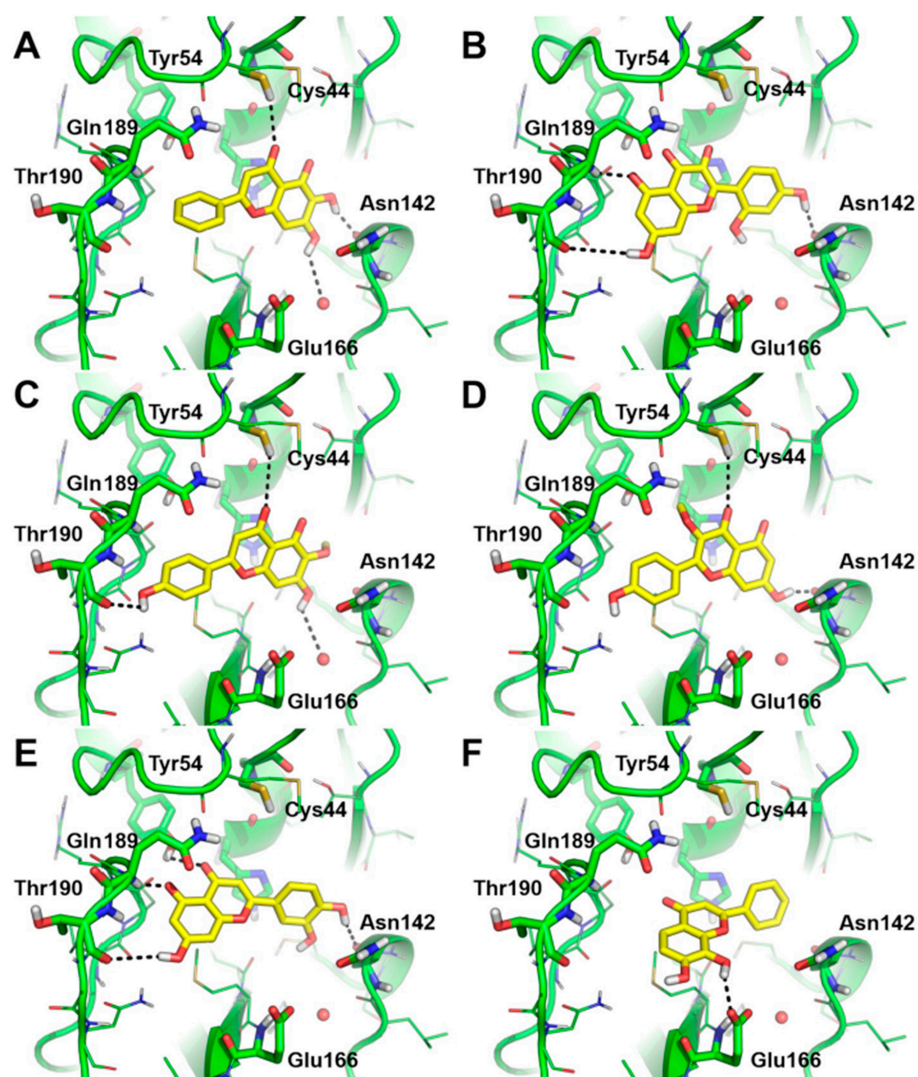


**Figure 3.** Putative binding modes of the bioactive natural products investigated in this work within the catalytic site of SARS-CoV-2 3CLpro, as predicted by molecular docking simulations. (A) Baicalein; (B) Morin; (C) Hispidulin; (D) Isokaempferide; (E) Luteolin; and (F) 7,8-dihydroxyflavone. The protein is shown as a green cartoon and lines (only residues within 6 Å from the ligands are shown, the others are omitted). The ligand polar contacts are highlighted by black dashed lines. The residues contacted by the ligands are labeled. Natural products are shown as yellow sticks, and non-polar H atoms are omitted.

#### 4. Discussion

The COVID-19 pandemic has revealed the urgent need for novel antiviral drugs. Flavonoids have been largely studied as possible inhibitors of 3CLpro and several studies found them to be active against SARS-CoV and MERS-CoV proteases [19]. It has previously been shown that several of these compounds can impair HCoV-229E replication in vitro [63]. The antiviral activity of Quercetin was previously observed in vitro against HSV-1 [64] and during in vitro and in vivo Rhinovirus infection [65], and its derivatives also show antiviral activity against Respiratory Syncytial Virus (RSV) [66] and Influenza A H1N1 virus replication in cell cultures [67]. During the COVID-19 pandemic, many flavonoids were examined against SARS-CoV-2 3CLpro. In particular, it has been observed that myricetin covalently binds to the Cys300 and Cys41 of 3CLpro [68].

In this study, we identified in silico flavonoid derivatives and subsequently evaluated a library of flavonoid derivatives for their inhibitory activity on 3CLpro. Firstly, we identified

Morin, Baicalein, Hispidulin, Taxifolin, Steppogenin, Quercetin, Chrysin, Sakuranetin, Alnus, Galangin, Isosakuranetin, and Isokaempferide through in silico analyses.

Then, we tested these flavonoids in a 3CLpro enzymatic assay, finding four of them, Morin, Baicalein, Hispidulin, and Isokaempferide, to be active against 3CLpro. Baicalein, the most promising compound, inhibited 3CLpro activity above 90%, and Morin, Hispidulin, and Isokaempferide were partially active against SARS-CoV-2 3CLpro. The antiviral activity of Morin was observed against the *Herpesviridae* family [69], whereas Hispidulin has been associated with Influenza A H1N1 neuraminidase inhibition [70].

In order to assess their anti-coronaviral activity, we tested these compounds against SARS-CoV-2 replication with an in vitro assay, but only Baicalein had more than 50% activity against virus replication at concentrations that were non-toxic for Vero E6 cells. In agreement, Seri et al. [4] found Baicalin, but also Herbacetin and Pectolarin, to be effective against SARS-CoV-2. Other studies have reported in vitro Baicalein to have antiviral activity against SARS-CoV-2 [71]. The anti-SARS-CoV-2 properties of Baicalein were, in part, explained through the observation of in silico interactions between this compound and 3CLpro [15,72]. Furthermore, a crystallographic picture of this molecular interaction was obtained with SARS-CoV-1 3CLpro [73], which has 96% similarity with SARS-CoV-2 [74].

Since the emergence of SARS-CoV-1 in 2002 [75], MERS-CoV in 2012 [76], and SARS-CoV-2 in 2019 [77], research has uncovered many details of the life cycle of coronavirus and its pathogenesis; however, there are currently no approved drugs with anti-pancoronaviral activity.

Thus, we extended our observations on the anti-SARS-CoV-2 activity of Baicalein, testing its inhibitory potency against additional members of the *Coronaviridae* family. To our knowledge, for the first time we found that this compound is highly active against F-CoV, B-CoV, and HCoV-OC43 replication. F-CoV [78,79] and HCoV-OC43 [80] have been previously used as SARS-CoV-2 surrogates in order to test the virucidal and antiviral activity of several compounds.

Considering that F-CoV belongs to the alpha coronavirus genus, Baicalein could be active against the human alpha Cov species, i.e., HCoV-229E which usually infects the upper respiratory tract, but can cause more severe diseases in newborns and in immunocompromised individuals [81], and HCoV-NL63 which causes bronchiolitis in infants [82] and pneumonia.

Furthermore, from a translation point of view, the activity of Baicalin against HCoV-OC43 is relevant. Indeed, this HCoV causes very mild disease in immunocompetent adults [81], but it is a threat for newborns (0–1 year) causing bronchiolitis [83].

The broad-spectrum of the anti-pancoronaviral action of Baicalein against F-CoV, B-CoV, and HCoV-OC43 could be explained by the fact that 3CLpro is highly conserved within the *Coronaviridae* family [74]. Of note, the anti-inflammatory activity of flavonoids has also been shown, modulating the expression of inflammatory markers, such as IL1-B and Tumor Necrosis Factor Alpha (TNF-a) [84], and it can modulate the NLRP3 inflammasome [85,86]. Interestingly, IL1-B and TNF-a blood levels were associated with post-COVID-19 illness [87] and the use of flavonoid-derived compounds could mitigate post-COVID-19 symptoms.

In this context, Baicalein has been shown to interact with the NLRP3 inflammasome [86] and with Nf-kB through Nrf2 activation [88].

The limitations of this study include a lack of other HCoV models, including low (HCoV-NL63 and HKU1) and high (MERS-CoV) human pathogenetic coronavirus, but also additional animal coronaviruses (bat coronaviruses) in order to confirm the anti-pancoronaviral activity of Baicalein. The availability of a compound with proven activity against emerging coronaviruses would represent great value as coronaviruses infecting animals still represent a threat. Indeed, a novel CoV infecting pigs, named swine acute diarrhea syndrome (SADS)-CoV that recently caused an outbreak in China [89], is capable of infecting human derived cells [90], suggesting that it might also be capable of jumping to humans.

Moreover, several compounds were found to be toxic for the cells and were tested against SARS-CoV-2 in low concentrations. The latter could have underestimated the evaluation of the antiviral potency of these molecules and indicates the need to improve the synthesis processes and test new Baicalein-derived compounds against coronaviruses.

In conclusion, our study confirmed the *in vitro* antiviral activity of Baicalein against SARS-CoV-2 replication, but also demonstrated clear evidence of the anti-pan-coronaviral activity exerted by this compound. Given that Baicalein and the other bioactive compounds highlighted in this work belong to a very large family of natural compounds, this work paves the way for the exploration of naturally occurring flavonoids in the identification of additional and effective 3CLpro inhibitors of SARS-CoV-2 replication. Starting from our results, future investigations are warranted in order to elucidate the possible activity of Baicalein and its derivatives against other steps of the coronavirus life cycle. Furthermore, we underline the importance of using an experimental approach combining *in silico* and *in vitro* analyses in order to uncover novel antiviral drugs that are suitable for treating SARS-CoV-2 in this current pandemic or for the next emerging viral pathogen.

**Author Contributions:** Conceptualization, M.M., D.Q., L.S. and A.P.; Methodology, M.M., D.Q., A.C., F.G., L.S., S.C., M.F., A.D., F.F. and N.C.; Investigation, A.C., F.G., L.S., S.C., M.F., A.D., F.F., E.C. and N.C.; Writing—original draft, M.M., D.Q., L.S., A.P. and C.S.; Writing—review & editing, N.C., N.M., B.B., G.A., A.P. and C.S.; Supervision, N.C., N.M., B.B., G.A., A.P. and C.S. All authors have read and agreed to the published version of the manuscript.

**Funding:** This work was supported by a grant from Sapienza University (ATENEO H2020, PH120172-B4BA8CAF) to A.G. Funding sources were not involved in the study design; in the collection, analysis and interpretation of data; in the writing of this manuscript; and in the decision to submit the article for publication.

**Institutional Review Board Statement:** Not applicable.

**Informed Consent Statement:** Not applicable.

**Data Availability Statement:** The datasets analysed during this study are available from the corresponding author on reasonable request.

**Conflicts of Interest:** The authors declare no conflict of interest.

## References

1. Hui, D.S.; Azhar, E.; Madani, T.A.; Ntoumi, F.; Kock, R.; Dar, O.; Ippolito, G.; Mchugh, T.D.; Memish, Z.A.; Drosten, C.; et al. The continuing 2019-nCoV epidemic threat of novel coronaviruses to global health—The latest 2019 novel coronavirus outbreak in Wuhan, China. *Int. J. Infect. Dis.* **2020**, *91*, 264–266. [[CrossRef](#)] [[PubMed](#)]
2. Wu, F.; Zhao, S.; Yu, B.; Chen, Y.M.; Wang, W.; Song, Z.G.; Hu, Y.; Tao, Z.W.; Tian, J.H.; Pei, Y.Y.; et al. A new coronavirus associated with human respiratory disease in China. *Nature* **2020**, *579*, 265–269. [[CrossRef](#)] [[PubMed](#)]
3. Tsai, S.C.; Lu, C.C.; Bau, D.T.; Chiu, Y.J.; Yen, Y.T.; Hsu, Y.M.; Fu, C.W.; Kuo, S.C.; Lo, Y.S.; Chiu, H.Y.; et al. Approaches towards fighting the COVID-19 pandemic (Review). *Int. J. Mol. Med.* **2021**, *47*, 3–22. [[CrossRef](#)]
4. Jo, S.; Kim, S.; Kim, D.Y.; Kim, M.S.; Shin, D.H. Flavonoids with inhibitory activity against SARS-CoV-2 3CLpro. *J. Enzyme Inhib. Med. Chem.* **2020**, *35*, 1539–1544. [[CrossRef](#)]
5. Rehman, M.T.; AlAjmi, M.F.; Hussain, A. Natural Compounds as Inhibitors of SARS-CoV-2 Main Protease (3CLpro): A Molecular Docking and Simulation Approach to Combat COVID-19. *Curr Pharm Des.* **2021**, *27*, 3577–3589. [[CrossRef](#)]
6. Chen, Y.; Liu, Q.; Guo, D. Emerging coronaviruses: Genome structure, replication, and pathogenesis. *J. Med. Virol.* **2020**, *92*, 418–423. [[CrossRef](#)] [[PubMed](#)]
7. Jin, Z.; Du, X.; Xu, Y.; Deng, Y.; Liu, M.; Zhao, Y.; Zhang, B.; Li, X.; Zhang, L.; Peng, C.; et al. Structure of Mpro from SARS-CoV-2 and discovery of its inhibitors. *Nature* **2020**, *582*, 289–293. [[CrossRef](#)]
8. Remuzzi, G.; Schiaffino, S.; Santoro, M.G.; FitzGerald, G.A.; Melino, G.; Patrono, C. Drugs for the prevention and treatment of COVID-19 and its complications: An update on what we learned in the past 2 years. *Front. Pharmacol.* **2020**, *13*, 987816. [[CrossRef](#)]
9. Jayk Bernal, A.; Gomes da Silva, M.M.; Musungaie, D.B.; Kovalchuk, E.; Gonzalez, A.; Delos Reyes, V.; Martín-Quirós, A.; Caraco, Y.; Williams-Diaz, A.; Brown, M.L.; et al. Molnupiravir for Oral Treatment of COVID-19 in Nonhospitalized Patients. *N. Engl. J. Med.* **2022**, *386*, 509–520. [[CrossRef](#)]
10. Akinosoglou, K.; Schinas, G.; Gogos, C. Oral Antiviral Treatment for COVID-19: A Comprehensive Review on Nirmaxvir/Ritonavir. *Viruses* **2022**, *14*, 2540. [[CrossRef](#)]

11. Vangeel, L.; Chiu, W.; De Jonghe, S.; Maes, P.; Slechten, B.; Raymenants, J.; André, E.; Leyssen, P.; Neyts, J.; Jochmans, D. Remdesivir, Molnupiravir and Nirmatrelvir remain active against SARS-CoV-2 Omicron and other variants of concern. *Antivir. Res.* **2022**, *198*, 105252. [[CrossRef](#)] [[PubMed](#)]
12. Rubin, R. From Positive to Negative to Positive Again—The Mystery of Why COVID-19 Rebounds in Some Patients Who Take Paxlovid. *JAMA* **2022**, *327*, 2380–2382. [[CrossRef](#)]
13. Russo, M.; Moccia, S.; Spagnuolo, C.; Tedesco, I.; Russo, G.L. Roles of flavonoids against coronavirus infection. *Chem. Biol. Interact.* **2020**, *328*, 109211. [[CrossRef](#)]
14. Clementi, N.; Scagnolari, C.; D'Amore, A.; Palombi, F.; Criscuolo, E.; Frasca, F.; Pierangeli, A.; Mancini, N.; Antonelli, G.; Clementi, M.; et al. Naringenin is a powerful inhibitor of SARS-CoV-2 infection in vitro. *Pharmacol. Res.* **2021**, *163*, 105255. [[CrossRef](#)]
15. Kaul, R.; Paul, P.; Kumar, S.; Büsselberg, D.; Dwivedi, V.D.; Chaari, A. Promising Antiviral Activities of Natural Flavonoids against SARS-CoV-2 Targets: Systematic Review. *Int. J. Mol. Sci.* **2021**, *22*, 11069. [[CrossRef](#)]
16. Maleki, S.J.; Crespo, J.F.; Cabanillas, B. Anti-inflammatory effects of flavonoids. *Food Chem.* **2019**, *299*, 125124. [[CrossRef](#)]
17. Theoharides, T.C.; Cholevas, C.; Polyzoidis, K.; Politis, A. Long-COVID syndrome-associated brain fog and chemofog: Luteolin to the rescue. *Biofactors* **2021**, *47*, 232–241. [[CrossRef](#)]
18. Bardelčíková, A.; Miroššay, A.; Šoltýs, J.; Mojžiš, J. Therapeutic and prophylactic effect of flavonoids in post-COVID-19 therapy. *Phytother. Res.* **2022**, *36*, 2042–2060. [[CrossRef](#)]
19. Jo, S.; Kim, H.; Kim, S.; Shin, D.H.; Kim, M.S. Characteristics of flavonoids as potent MERS-CoV 3C-like protease inhibitors. *Chem. Biol. Drug Des.* **2019**, *94*, 2023–2030. [[CrossRef](#)] [[PubMed](#)]
20. Theerawatanasirikul, S.; Thangthamniyom, N.; Kuo, C.J.; Semkum, P.; Phecharat, N.; Chankeeree, P.; Lekcharoensuk, P. Natural Phytochemicals, Luteolin and Isoginkgetin, Inhibit 3C Protease and Infection of FMDV, In Silico and In Vitro. *Viruses* **2021**, *13*, 2118. [[CrossRef](#)] [[PubMed](#)]
21. Ghirga, F.; Quaglio, D.; Mori, M.; Cammarone, S.; Iazzetti, A.; Goggiamani, A.; Ingallina, C.; Botta, B.; Calcaterra, A. A unique high-diversity natural product collection as a reservoir of new therapeutic leads. *Org. Chem. Front.* **2021**, *8*, 996–1025. [[CrossRef](#)]
22. Angiosperm Phylogeny, G.; Chase, M.W.; Christenhusz, M.J.M.; Fay, M.F.; Byng, J.W.; Judd, W.S.; Soltis, D.E.; Mabberley, D.J.; Sennikov, A.N.; Soltis, P.S. An update of the Angiosperm Phylogeny Group classification for the orders and families of flowering plants: APG IV. *Bot. J. Linn. Soc.* **2016**, *181*, 1–20. [[CrossRef](#)]
23. Wiczkowski, W.; Romaszko, J.; Bucinski, A.; Szawara-Nowak, D.; Honke, J.; Zielinski, H.; Piskula, M.K. Quercetin from shallots (*Allium cepa* L. var. *aggregatum*) is more bioavailable than its glucosides. *J. Nutr.* **2008**, *138*, 885–888. [[CrossRef](#)] [[PubMed](#)]
24. Häkkinen, S.H.; Kärenlampi, S.O.; Heinonen, I.M.; Mykkänen, H.M.; Törrönen, A.R. Content of the flavonols quercetin, myricetin, and kaempferol in 25 edible berries. *J. Agric. Food Chem.* **1999**, *47*, 2274–2279. [[CrossRef](#)]
25. Sakawa, Y. Chemical constituents of *Alnus sieboldiana* (Betulaceae) II. The isolation and structure of flavonoids and stilbenes. *BCSJ* **1971**, *44*, 2761–2766.
26. Moghaddam, G.; Ebrahimi, S.A.; Rahbar-Roshandel, N.; Foroumadi, A. Antiproliferative activity of flavonoids: Influence of the sequential methoxylation state of the flavonoid structure. *Phytother. Res.* **2012**, *26*, 1023–1028. [[CrossRef](#)]
27. Bradburn, M.J.; Clark, T.G.; Love, S.B.; Altman, D.G. Survival analysis Part III: Multivariate data analysis—choosing a model and assessing its adequacy and fit. *Br. J. Cancer* **2003**, *89*, 605–611. [[CrossRef](#)]
28. Arbos, P.; Arango, M.A.; Campanero, M.A.; Irache, J.M. Quantification of the bioadhesive properties of protein-coated PVM/MA nanoparticles. *Int. J. Pharm.* **2002**, *242*, 129–136. [[CrossRef](#)]
29. Kaur, A.; Singh, R.; Dey, C.S.; Sharma, S.S.; Bhutani, K.K.; Singh, I.P. Antileishmanial phenylpropanoids from *Alpinia galanga* (Linn.) Willd. *Indian J. Exp. Biol.* **2010**, *48*, 314–317.
30. Sotnikova, O.M.; Chagovets, R.K.; Litvinenko, V.I. New flavanone compounds from *Euphorbia stepposa*. *Chem. Nat. Compd.* **1968**, *4*, 71–74. [[CrossRef](#)]
31. Beutler, J.A.; Cardellina II, J.H.; Lin, C.M.; Hamel, E.; Cragg, G.M.; Boyd, M.R. Centaureidin, a cytotoxic flavone from *Polymnia fruticosa*, inhibits tubulin polymerization. *Bioorg. Med. Chem. Lett.* **1993**, *3*, 581–584. [[CrossRef](#)]
32. Wagner, H.; Hörhammer, L.; Aurnhammer, G.; Farkas, L. Strukturklärung und Synthese des Didymins, eines Isosakuranetin-7- $\beta$ -rutinosids aus *Monarda didyma* L. *Chem. Ber.* **1968**, *101*, 445–449. [[CrossRef](#)]
33. Sowndhararajan, K.; Deepa, P.; Kim, M.; Park, S.J.; Kim, S. Baicalein as a potent neuroprotective agent: A review. *Biomed. Pharmacother.* **2017**, *95*, 1021–1032. [[CrossRef](#)] [[PubMed](#)]
34. Fu, C.X.; Xu, Y.J.; Zhao, D.X.; Ma, F.S. A comparison between hairy root cultures and wild plants of *Saussurea involucreta* in phenylpropanoids production. *Plant Cell Rep.* **2006**, *24*, 750–754. [[CrossRef](#)]
35. Siraichi, J.T.G.; Felipe, D.F.; Brambilla, L.Z.S.; Gatto, M.J.; Terra, V.A.; Cecchini, A.L.; Cortez, L.E.R.; Rodrigues-Filho, E.; Cortez, D.A.G. Antioxidant capacity of the leaf extract obtained from *Arrabidaea chica* cultivated in Southern Brazil. *PLoS ONE* **2013**, *8*, e72733. [[CrossRef](#)] [[PubMed](#)]
36. Mani, R.; Natesan, V. Chrysin: Sources, beneficial pharmacological activities, and molecular mechanism of action. *Phytochemistry* **2018**, *145*, 187–196. [[CrossRef](#)]
37. Asmi, K.S.; Lakshmi, T.; Balusamy, S.R.; Parameswari, R. Therapeutic aspects of taxifolin—An update. *J. Adv. Pharm. Res.* **2017**, *7*, 187–189.

38. Halevas, E.; Mavroidi, B.; Kaplanis, M.; Hatzidimitriou, A.G.; Moschona, A.; Litsardakis, G.; Pelecanou, M. Hydrophilic bis-MPA hyperbranched dendritic scaffolds as nanocarriers of a fully characterized flavonoid morin-Zn (II) complex for anticancer applications. *J. Inorg. Biochem.* **2022**, *232*, 111832. [[CrossRef](#)] [[PubMed](#)]
39. Kim, S.M.; Kang, K.; Jho, E.H.; Jung, Y.J.; Nho, C.W.; Um, B.H.; Pan, C.H. Hepatoprotective effect of flavonoid glycosides from *Lespedeza cuneata* against oxidative stress induced by tert-butyl hydroperoxide. *Phytother. Res.* **2011**, *25*, 1011–1017. [[CrossRef](#)]
40. Wollenweber, E.; Mann, K.; Arriaga-Giner, F.J.; Roitman, J.N.; West, J.G. Exudate flavonoids from two Australian Asteraceae, *Bracteantha viscosa* and *Cassinia quinquefaria*. *Phytochemistry* **1993**, *33*, 871–873. [[CrossRef](#)]
41. Yang, H.; Gan, C.; Guo, Y.; Qu, L.; Ma, S.; Ren, Y.; Wang, X.; Wang, L.; Huang, J.; Wang, J. Two novel compounds from green walnut husks (*Juglans mandshurica* Maxim.). *Nat. Prod. Res.* **2022**, *36*, 3389–3395. [[CrossRef](#)] [[PubMed](#)]
42. Kim, S.; Li, Y.; Lin, L.; Sayasith, P.R.; Tarr, A.T.; Wright, E.B.; Yasmin, S.; Lannigan, D.A.; O'Doherty, G.A. Synthesis and Biological Evaluation of 4'-Substituted Kaempfer-3-ols. *J. Org. Chem.* **2020**, *85*, 4279–4288. [[CrossRef](#)]
43. Li, H.X.; Park, J.U.; Su, X.D.; Kim, K.T.; Kang, J.S.; Kim, Y.R.; Kim, Y.H.; Yang, S.Y. Identification of anti-melanogenesis constituents from *Morus alba* L. leaves. *Molecules* **2018**, *23*, 2559. [[CrossRef](#)]
44. Kirubakaran, P.; Muthusamy, K.; Dhanachandra Singh, K.; Nagamani, S. Homology modeling, molecular dynamics, and molecular docking studies of *Trichomonas vaginalis* carbamate kinase. *Med. Chem. Res.* **2012**, *21*, 2105–2116. [[CrossRef](#)]
45. Zahran, E.M.; Abdelmohsen, U.R.; Hussein, A.S.; Salem, M.A.; Khalil, H.E.; Yehia Desoukey, S.; Fouad, M.A.; Kamel, M.S. Antitumor potential and molecular docking of flavonoids from *Ocimum forskolei* Benth. family Lamiaceae. *Nat. Prod. Res.* **2021**, *35*, 1933–1937. [[CrossRef](#)]
46. Meng, Q.; Li, G.; Luo, B.; Wang, L.; Lu, Y.; Liu, W. Screening and isolation of natural antioxidants from *Ziziphora clinopodioides* Lam. with high performance liquid chromatography coupled to a post-column Ce (IV) reduction capacity assay. *RSC Adv.* **2016**, *6*, 62378–62384. [[CrossRef](#)]
47. Chen, L.C.; Hsu, K.C.; Chiou, L.C.; Tseng, H.J.; Huang, W.J. Total synthesis and metabolic stability of hispidulin and its d-labelled derivative. *Molecules* **2017**, *22*, 1897. [[CrossRef](#)]
48. Singh, M.; Kaur, M.; Vyas, B.; Silakari, O. Design, synthesis and biological evaluation of 2-Phenyl-4H-chromen-4-one derivatives as polyfunctional compounds against Alzheimer's disease. *Med. Chem. Res.* **2018**, *27*, 520–530. [[CrossRef](#)]
49. Xu, S.; Shang, M.Y.; Liu, G.X.; Xu, F.; Wang, X.; Shou, C.C.; Cai, S.Q. Chemical constituents from the rhizomes of *Smilax glabra* and their antimicrobial activity. *Molecules* **2013**, *18*, 5265–5287. [[CrossRef](#)] [[PubMed](#)]
50. Douangamath, A.; Fearon, D.; Gehrtz, P.; Krojer, T.; Lukacik, P.; Owen, C.D.; Resnick, E.; Strain-Damerell, C.; Aimon, A.; Abranyi-Balog, P.; et al. Crystallographic and electrophilic fragment screening of the SARS-CoV-2 main protease. *Nat. Commun.* **2020**, *11*, 5047. [[CrossRef](#)] [[PubMed](#)]
51. Picarazzi, F.; Zuanon, M.; Pasqualetto, G.; Cammarone, S.; Romeo, I.; Young, M.T.; Brancale, A.; Bassetto, M.; Mori, M. Identification of Small Molecular Chaperones Binding P23H Mutant Opsin through an In Silico Structure-Based Approach. *J. Chem. Inf. Model* **2022**, *62*, 5794–5805. [[CrossRef](#)]
52. Platella, C.; Ghirga, F.; Zizza, P.; Pompili, L.; Marzano, S.; Pagano, B.; Quaglio, D.; Vergine, V.; Cammarone, S.; Botta, B.; et al. Identification of Effective Anticancer G-Quadruplex-Targeting Chemotypes through the Exploration of a High Diversity Library of Natural Compounds. *Pharmaceutics* **2020**, *13*, 1611. [[CrossRef](#)]
53. Kuchlyan, J.; Martinez-Fernandez, L.; Mori, M.; Gavvala, K.; Ciaco, S.; Boudier, C.; Richert, L.; Didier, P.; Tor, Y.; Improta, R.; et al. What Makes Thienoguanosine an Outstanding Fluorescent DNA Probe? *J. Am. Chem. Soc.* **2020**, *142*, 16999–17014. [[CrossRef](#)] [[PubMed](#)]
54. OEDOCKING 3.3.0.3: OpenEye Scientific Software, Inc. Santa Fe, NM. Available online: <http://www.eyesopen.com> (accessed on 27 December 2022).
55. McGann, M. FRED Pose Prediction and Virtual Screening Accuracy. *J. Chem. Inf. Model.* **2011**, *51*, 578–596. [[CrossRef](#)]
56. Hawkins, P.C.D.; Skillman, A.G.; Warren, G.L.; Ellingson, B.A.; Stahl, M.T. Conformer Generation with OMEGA: Algorithm and Validation Using High Quality Structures from the Protein Databank and the Cambridge Structural Database. *J. Chem. Inf. Model* **2010**, *50*, 572–584. [[CrossRef](#)]
57. QUACPAC 2.0.0.3: OpenEye Scientific Software, Santa Fe, NM. Available online: <http://www.eyesopen.com> (accessed on 27 December 2022).
58. SZYBKI 1.10.0.3: OpenEye Scientific Software, Santa Fe, NM. Available online: <http://www.eyesopen.com> (accessed on 27 December 2022).
59. Criscuolo, E.; Giuliani, B.; Ferrari, D.; Ferrarese, R.; Diotti, R.A.; Clementi, M.; Mancini, N.; Clementi, N. Proper Selection of In Vitro Cell Model Affects the Characterization of the Neutralizing Antibody Response against SARS-CoV-2. *Viruses* **2022**, *14*, 1232. [[CrossRef](#)]
60. Romeo, A.; Iacovelli, F.; Scagnolari, C.; Scordio, M.; Frasca, F.; Condò, R.; Ammendola, S.; Gaziano, R.; Anselmi, M.; Divizia, M.; et al. Potential Use of Tea Tree Oil as a Disinfectant Agent against Coronaviruses: A Combined Experimental and Simulation Study. *Molecules* **2022**, *27*, 3786. [[CrossRef](#)]
61. Kashyap, P.; Thakur, M.; Singh, N.; Shikha, D.; Kumar, S.; Baniwal, P.; Yadav, Y.S.; Sharma, M.; Sridhar, K.; Inbaraj, B.S. In Silico Evaluation of Natural Flavonoids as a Potential Inhibitor of Coronavirus Disease. *Molecules* **2022**, *27*, 6374. [[CrossRef](#)] [[PubMed](#)]

62. Pillaiyar, T.; Manickam, M.; Namasivayam, V.; Hayashi, Y.; Jung, S.H. An overview of Severe Acute Respiratory Syndrome-Coronavirus (SARS-CoV) 3CL protease inhibitors: Peptidomimetics and Small Molecule Chemotherapy. *J. Med. Chem.* **2016**, *59*, 6595–6628. [[CrossRef](#)]
63. Zhu, Y.; Scholle, F.; Kisthardt, S.C.; Xie, D.Y. Flavonols and dihydroflavonols inhibit the main protease activity of SARS-CoV-2 and the replication of human coronavirus 229E. *Virology* **2022**, *571*, 21–33. [[CrossRef](#)] [[PubMed](#)]
64. Lee, S.; Lee, H.H.; Shin, Y.S.; Kang, H.; Cho, H. The anti-HSV-1 effect of quercetin is dependent on the suppression of TLR-3 in Raw 264.7 cells. *Arch. Pharm. Res.* **2017**, *40*, 623–630. [[CrossRef](#)]
65. Ganesan, S.; Faris, A.N.; Comstock, A.T.; Wang, Q.; Nanua, S.; Hershenson, M.B.; Sajjan, U.S. Quercetin inhibits rhinovirus replication in vitro and in vivo. *Antivir. Res.* **2012**, *94*, 258–271. [[CrossRef](#)]
66. Lopes, B.R.P.; da Costa, M.F.; Genova Ribeiro, A.; da Silva, T.F.; Lima, C.S.; Caruso, I.P.; de Araujo, G.C.; Kubo, L.H.; Iacovelli, F.; Falconi, M.; et al. Quercetin pentaacetate inhibits in vitro human respiratory syncytial virus adhesion. *Virus Res.* **2020**, *276*, 197805. [[CrossRef](#)]
67. Mehrbod, P.; Abdalla, M.A.; Fotouhi, F.; Heidarzadeh, M.; Aro, A.O.; Eloff, J.N.; McGaw, L.J.; Fasina, F.O. Immunomodulatory properties of quercetin-3-O- $\alpha$ -L-rhamnopyranoside from *Rapanea melanophloeos* against influenza A virus. *BMC Complement. Altern. Med.* **2018**, *18*, 184. [[CrossRef](#)]
68. Xiong, Y.; Zhu, G.H.; Zhang, Y.N.; Hu, Q.; Wang, H.N.; Yu, H.N.; Qin, X.Y.; Guan, X.Q.; Xiang, Y.W.; Tang, H.; et al. Flavonoids in *Ampelopsis grossedentata* as covalent inhibitors of SARS-CoV-2 3CLpro: Inhibition potentials, covalent binding sites and inhibitory mechanisms. *Int J. Biol. Macromol.* **2021**, *187*, 976–987. [[CrossRef](#)] [[PubMed](#)]
69. Gravina, H.D.; Tafuri, N.F.; Silva Júnior, A.; Fietto, J.L.; Oliveira, T.T.; Diaz, M.A.; Almeida, M.R. In vitro assessment of the antiviral potential of trans-cinnamic acid, quercetin and morin against equid herpesvirus 1. *Res. Vet. Sci.* **2011**, *91*, e158–e162. [[CrossRef](#)]
70. Bang, S.; Quy Ha, T.K.; Lee, C.; Li, W.; Oh, W.K.; Shim, S.H. Antiviral activities of compounds from aerial parts of *Salvia plebeia* R. Br. *J. Ethnopharmacol.* **2016**, *192*, 398–405. [[CrossRef](#)]
71. Liu, H.; Ye, F.; Sun, Q.; Liang, H.; Li, C.; Li, S.; Lu, R.; Huang, B.; Tan, W.; Lai, L. *Scutellaria baicalensis* extract and baicalein inhibit replication of SARS-CoV-2 and its 3C-like protease in vitro. *J. Enzyme Inhib. Med. Chem.* **2021**, *36*, 497–503. [[CrossRef](#)] [[PubMed](#)]
72. Onyango, H.; Odhiambo, P.; Angwenyi, D.; Okoth, P. In Silico Identification of New Anti-SARS-CoV-2 Main Protease (Mpro) Molecules with Pharmacokinetic Properties from Natural Sources Using Molecular Dynamics (MD) Simulations and Hierarchical Virtual Screening. *J. Trop. Med.* **2022**, *2022*, 3697498. [[CrossRef](#)] [[PubMed](#)]
73. Feng, J.; Li, D.; Zhang, J.; Yin, X.; Li, J. Crystal structure of SARS-CoV 3C-like protease with baicalein. *Biochem. Biophys. Res. Commun.* **2022**, *611*, 190–194. [[CrossRef](#)] [[PubMed](#)]
74. Iketani, S.; Hong, S.J.; Sheng, J.; Bahari, F.; Culbertson, B.; Atanaki, F.F.; Aditham, A.K.; Kratz, A.F.; Luck, M.I.; Tian, R.; et al. Functional map of SARS-CoV-2 3CL protease reveals tolerant and immutable sites. *Cell Host Microbe* **2022**, *30*, 1354–1362. [[CrossRef](#)]
75. Drosten, C.; Günther, S.; Preiser, W.; van der Werf, S.; Brodt, H.R.; Becker, S.; Rabenau, H.; Panning, M.; Kolesnikova, L.; Fouchier, R.A.; et al. Identification of a novel coronavirus in patients with severe acute respiratory syndrome. *N. Engl. J. Med.* **2003**, *348*, 1967–1976. [[CrossRef](#)] [[PubMed](#)]
76. Bermingham, A.; Chand, M.A.; Brown, C.S.; Aarons, E.; Tong, C.; Langrish, C.; Hoschler, K.; Brown, K.; Galiano, M.; Myers, R.; et al. Severe respiratory illness caused by a novel coronavirus, in a patient transferred to the United Kingdom from the Middle East, September 2012. *Euro. Surveill.* **2012**, *17*, 20290. [[CrossRef](#)]
77. Ciotti, M.; Angeletti, S.; Minieri, M.; Giovannetti, M.; Benvenuto, D.; Pascarella, S.; Sagnelli, C.; Bianchi, M.; Bernardini, S.; Ciccozzi, M. COVID-19 Outbreak: An Overview. *Chemotherapy* **2019**, *64*, 215–223. [[CrossRef](#)]
78. Camero, M.; Lanave, G.; Catella, C.; Lucente, M.S.; Decaro, N.; Martella, V.; Buonavoglia, C. Evaluation of virucidal activity of fabrics using feline coronavirus. *J. Virol. Methods* **2021**, *295*, 114214. [[CrossRef](#)]
79. Vuong, W.; Khan, M.B.; Fischer, C.; Arutyunova, E.; Lamer, T.; Shields, J.; Saffran, H.A.; McKay, R.T.; van Belkum, M.J.; Joyce, M.A.; et al. Feline coronavirus drug inhibits the main protease of SARS-CoV-2 and blocks virus replication. *Nat. Commun.* **2020**, *11*, 4282. [[CrossRef](#)] [[PubMed](#)]
80. Bhavanam, S.; Lee, B.; Qiu, Y.; Zelyas, N.; Pang, X.L. Evaluation of compressed sodium chloride on the inactivation of SARS-CoV-2 and surrogates. *PLoS ONE* **2022**, *17*, e0277881. [[CrossRef](#)]
81. Gorse, G.J.; Donovan, M.M.; Patel, G.B.; Balasubramanian, S.; Lusk, R.H. Coronavirus and Other Respiratory Illnesses Comparing Older with Young Adults. *Am. J. Med.* **2015**, *128*, 11–20. [[CrossRef](#)] [[PubMed](#)]
82. Ebihara, T.; Endo, R.; Ma, X.; Ishiguro, N.; Kikuta, H. Detection of human coronavirus NL63 in young children with bronchiolitis. *J. Med. Virol.* **2005**, *75*, 463–465. [[CrossRef](#)]
83. Tsou, P.; Vadivelan, A.; Kovvuri, M.; Garg, N.; Thangavelu, M.; Wang, Y.; Raj, S. Association between multiple respiratory viral infections and pediatric intensive care unit admission among infants with bronchiolitis. *Arch. Pediatr.* **2020**, *27*, 39–44. [[CrossRef](#)]
84. Al-Khayri, J.M.; Sahana, G.R.; Nagella, P.; Joseph, B.V.; Alessa, F.M.; Al-Mssallem, M.Q. Flavonoids as Potential Anti-Inflammatory Molecules: A Review. *Molecules* **2022**, *27*, 2901. [[CrossRef](#)]
85. Saeedi-Boroujeni, A.; Mahmoudian-Sani, M.R. Anti-inflammatory potential of Quercetin in COVID-19 treatment. *J. Inflamm.* **2021**, *18*, 3. [[CrossRef](#)] [[PubMed](#)]

86. Rui, W.; Li, S.; Xiao, H.; Xiao, M.; Shi, J. Baicalein Attenuates Neuroinflammation by Inhibiting NLRP3/caspase-1/GSDMD Pathway in MPTP Induced Mice Model of Parkinson's Disease. *Int. J. Neuropsychopharmacol.* **2020**, *23*, 762–773. [[CrossRef](#)]
87. Schultheiß, C.; Willscher, E.; Paschold, L.; Gottschick, C.; Klee, B.; Henkes, S.S.; Bosurgi, L.; Dutzmann, J.; Sedding, D.; Frese, T.; et al. The IL-1 $\beta$ , IL-6, and TNF cytokine triad is associated with post-acute sequelae of COVID-19. *Cell Rep. Med.* **2022**, *3*, 100663. [[CrossRef](#)]
88. Dai, C.; Li, H.; Wang, Y.; Tang, S.; Velkov, T.; Shen, J. Inhibition of Oxidative Stress and ALOX12 and NF- $\kappa$ B Pathways Contribute to the Protective Effect of Baicalein on Carbon Tetrachloride-Induced Acute Liver Injury. *Antioxidants* **2021**, *10*, 976. [[CrossRef](#)] [[PubMed](#)]
89. Zhou, P.; Fan, H.; Lan, T.; Yang, X.; Shi, W.; Zhang, W.; Zhu, Y.; Zhang, Y.; Xie, Q.; Mani, S.; et al. Fatal swine acute diarrhoea syndrome caused by an HKU2-related coronavirus of bat origin. *Nature* **2018**, *556*, 255–258. [[CrossRef](#)] [[PubMed](#)]
90. Edwards, C.E.; Yount, B.L.; Graham, R.L.; Leist, S.R.; Hou, Y.J.; Dinno, K.H., 3rd; Sims, A.C.; Swanstrom, J.; Gully, K.; Scobey, T.D.; et al. Swine acute diarrhea syndrome coronavirus replication in primary human cells reveals potential susceptibility to infection. *Proc. Natl. Acad. Sci. USA* **2020**, *117*, 26915–26925. [[CrossRef](#)]

**Disclaimer/Publisher's Note:** The statements, opinions and data contained in all publications are solely those of the individual author(s) and contributor(s) and not of MDPI and/or the editor(s). MDPI and/or the editor(s) disclaim responsibility for any injury to people or property resulting from any ideas, methods, instructions or products referred to in the content.